12 MARCH 2007
Volume 90 Number 11

APPLIED PHYSICS LETTERS

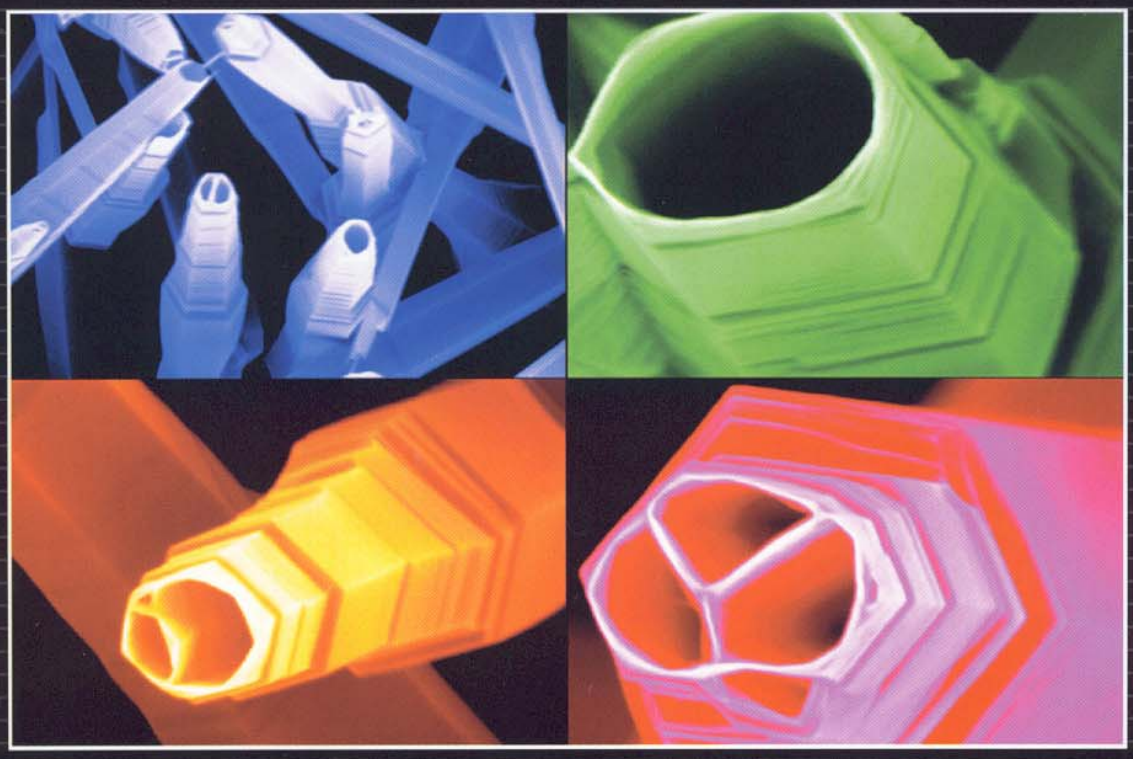

0003-6951(20070312)90:11;1-9

AMERICAN INSTITUTE OF PHYSICS

Formation of single crystalline ZnO nanotubes without catalysts and templates

Samuel L. Mensah and Vijaya K. Kayastha
Department of Physics, Michigan Technological University, 1400 Townsend Drive, Houghton, Michigan 49931

Ilia N. Ivanov and David B. Geohegan
Condensed Matter Sciences Division, Oak Ridge National Laboratory, Oak Ridge, Tennessee 37831

Yoke Khin Yap[a)]
Department of Physics, Michigan Technological University, 1400 Townsend Drive, Houghton, Michigan 49931

(Received 21 November 2006; accepted 10 January 2007; published online 13 March 2007)

Oxide and nitride nanotubes have gained attention for their large surface areas, wide energy band gaps, and hydrophilic natures for various innovative applications. These nanotubes were either grown by templates or multistep processes with uncontrollable crystallinity. Here the authors show that single crystal ZnO nanotubes can be directly grown on planar substrates without using catalysts and templates. These results are guided by the theory of nucleation and the vapor-solid crystal growth mechanism, which is applicable for transforming other nanowires or nanorods into nanotubular structures. © *2007 American Institute of Physics*. [DOI: 10.1063/1.2714186]

Oxide and nitride nanotubes are unique for their wide energy band gaps and hydrophilic natures, which are not available from carbon nanotubes. GaN,[1] silica,[2] ZnO,[3,4] and TiO_2 (Ref. 5) nanotubes have been synthesized by using multistep processes with templates or hydrothermal techniques. Some exciting applications including photochemical cells,[5] nanofluidic transistors,[6] and DNA sensors[7] have been demonstrated with the use of these nanotubes. Among these materials, ZnO nanotubes have generated significant interests due to their multifunctional properties. Various ZnO nanostructures have been reported including nanowires[8,9] and nanobelts[10] for their electronic,[11,12] optics,[13] mechanical,[14] and piezoelectric[15] applications. ZnO nanotubes are expected to accomplish the uses of other ZnO nanostructures for applications at the cutting edge of nanoscale. These nanostructures will enable unique electronic, optical, photochemical, nanofluidic, biological, and chemical applications.

Crystal quality of these oxide and nitride nanotubes is important for their optimum physical properties and performance. Thus it is desired to establish basic understanding on the growth of single crystalline ZnO nanotubes using the conventional thermal chemical vapor deposition (CVD) technique. Based on the theory of nucleation and vapor-solid crystal growth, we have experimentally proven the direct growth of single crystalline ZnO nanotubes without the use of multiple processes, catalysts, or templates. According to the theory of nucleation, the probability of nuclei formation is given by[16,17] $P_N = A \exp(-\pi\sigma^2/k^2T^2 \ln \alpha)$, where A is a constant, σ is the surface energy, $\alpha - 1$ is the supersaturation, $\alpha = p/p_0$, p is the pressure of vapor, p_0 is the equilibrium vapor pressure of the condensed phase at that temperature, k is the Boltzmann constant, and T is the temperature in Kelvin. In addition, the binding energy of an ionic growth species (and generally for nonionic growth species too) on a substrate is given by[18] $E = \beta(q^2/a)$, where β is a numerical factor which depends on the site of the deposition, a is the lattice spacing, and q is the charge of the ion. These ions prefer to condense on locations with the maximum number of nearest neighbors. Thus for a growth surface with a step as shown in Fig. 1(a), ions prefer to condense at sites 6, 5, 1, 4, 2, and 3, according to sequence since $\beta_6 > \beta_5 > \beta_1 > \beta_4 > \beta_2 > \beta_3$.[18] Thus an atomically flat layer will always spread from the edges under conditions with sufficient surface energy.

For a flat two-dimensional (2D) growth surface without steps, only sites 1, 2, and 3 exist. In this case, higher binding energies at the edges (sites 1 and 2) will enable selective condensation of growth species at the edges. For ZnO, it is well known that the growth rate along the c axis is relatively faster.[8,9] At decreased growth temperatures, the nucleation probability P_N and the surface migration will be suppressed. Thus if the growth temperatures are low enough to suppress migration along the 2D surface of the c plane but high enough to sustain the growth along the c axis, the condensation and growth will be limited at the edges of the c plane of ZnO, as shown in Fig. 1(b). Under these conditions, the growth of ZnO nanotubes along the c axis will be possible. However, if steps or vacancies are found in locations beyond the edges, nucleation will also take place at these sites as shown in Fig. 1(c) due to their higher β values than those at the edges.

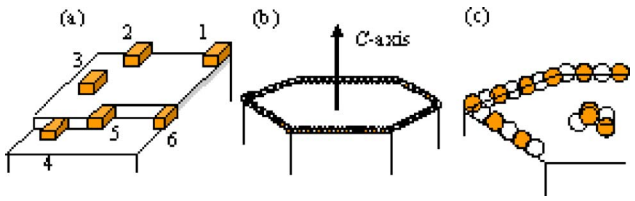

FIG. 1. (Color online) (a) Nucleation sites on a surface with a step. (b) Preferential condensation of growth species at the c-plane edges of a ZnO nanorod. (c) Addition nucleation beyond the edges when steps and vacancies are found.

[a)]Author to whom correspondence should be addressed; electronic mail: ykyap@mtu.edu

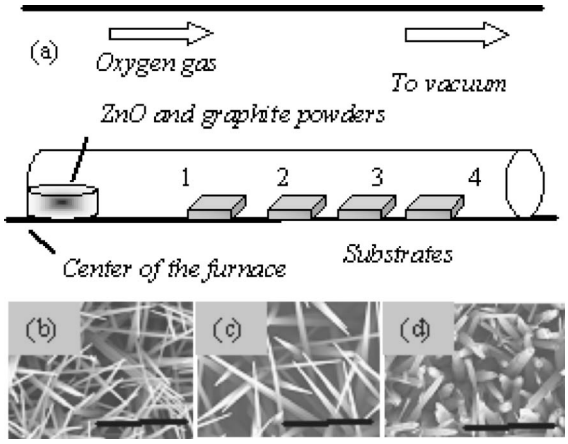

FIG. 2. (a) Experimental setup in a double-tube horizontal furnace. Appearance of ZnO nanorods on substrates (b) 2, (c) 3, and ZnO nanotubes on (d) substrate 4. The scale bars are 6 μm.

Based on this model, we have conducted a series of experiments to first start the growth of the *c* surfaces of ZnO nanorods and then decrease the growth temperatures for the formation of the ZnO nanotubes. The growth was performed in a horizontal furnace consisting of a quartz tube vacuum chamber. A smaller quartz tube (60 cm long and 2 cm in diameter) containing the precursor materials and the substrates was placed within the vacuum chamber. A mixture of ZnO (0.2 g) and graphite (0.1 g) powder in an alumina boat was used as the precursor materials. These are placed at the closed end of the smaller quartz tube, as shown in Fig. 2(a). A series of oxidized silicon substrates (1–4) was then placed downstream from the mixture in the small quartz tube. The small tube was then inserted into the vacuum chamber such that the closed end is at the center of the furnace. The temperature of the furnace was raised to 1100 °C. At ~350 °C, oxygen gas was introduced into the furnace at a flow rate of 40 SCCM (SCCM denotes cubic centimeter per minute at STP). The temperature was held at 1100 °C for 30 min and turned off to allow cooling to 600–700 °C in ~30 min. Then experiments are terminated by cooling the system to RT by opening the heating panel of the furnace. According to a calibration experiment, when the furnace is heated at 1100 °C, the temperatures of substrates 1–4 are about 700, 600, 500, and 420 °C, respectively. These temperatures will be lower as the furnace temperatures decrease from 1100 °C. After the growth, all samples were examined with scanning electron microscopy (SEM). In all experiments, no coating was formed on substrate 1. ZnO Nanorods with sharp tips were grown on substrates 2 and 3, as shown in Figs. 2(b) and 2(c), respectively. We detected ZnO nanotubes only on substrates 4, as shown in Fig. 2(d). The diameters of these nanotubes are between 80 and 500 nm near the opened tips.

The appearance of these ZnO nanotubes is highlighted in Fig. 3. Some of these nanotubes have single tubular channel, as shown in Figs. 3(a) and 3(b), which is as predicted by theory. As shown in Figs. 3(c) and 3(d), some of these nanotubes have multiple channels. The formation of these multichannel nanotubes is also expected by the nucleation model discussed earlier. During the nucleation and growth, steps or vacancies could be formed at locations beyond the edges, as shown in Fig. 1(c). Especially at suppressed growth temperatures, the formation of steps and vacancies will induce the formation of addition islands at these locations. These islands will tend to merge with the edges so as to reduce their surface energy (larger island, lower surface energy).[18] These processes are accompanied by the growth along the *c* axis and thus transform the single channel nanotubes to multichannel structures.

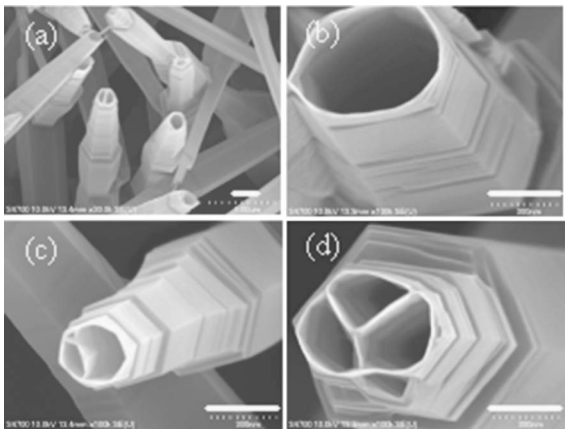

FIG. 3. Appearance of various ZnO nanotubes. The scale bars are 300 nm.

Obviously, the diameters of these ZnO nanotubes resembled those of the ZnO nanorods. Since the substrate surfaces are smooth as inspected by SEM (Hitachi S-4700, resolution of ~2.1 nm at 1 kV), the diameters of these nanotubes and nanorods (~80–600 nm) are unlikely to be determined by surface steps or roughness of the substrates. We anticipate that the diameters of the ZnO nanotubes can be controlled by the growth conditions including the partial vapor pressures and the growth temperatures.

Figure 4(a) shows the typical x-ray diffraction spectra of these nanotube samples. These spectra can be indexed for diffractions from the (002), (101), (102), and (103) planes of wurtzite crystals with lattice constants $a=0.325$ mm and $c=0.521$ nm, which are corresponding to ZnO. The predomi-

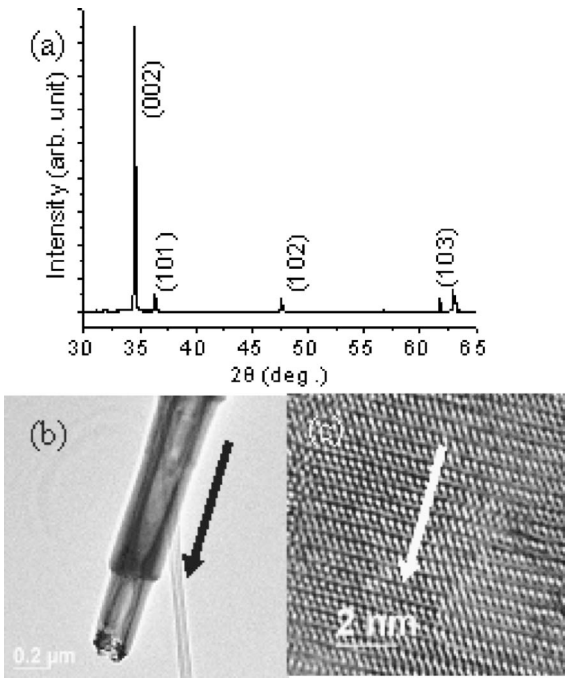

FIG. 4. (a) X-ray diffraction, (b) TEM, and (c) higy resolution TEM of a ZnO nanotubes. The arrows representing the tubular axes of these nanotubes.

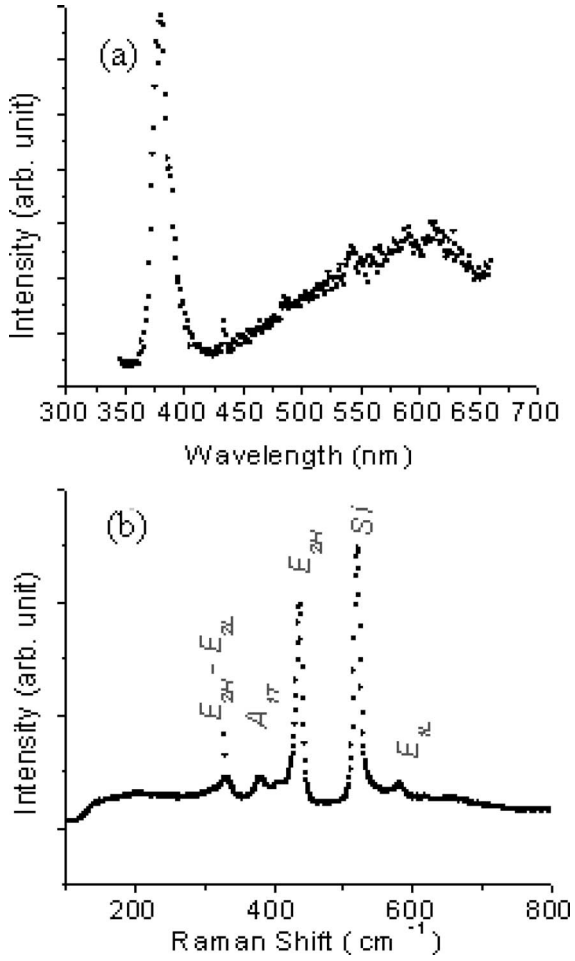

FIG. 5. (a) Raman scattering and (b) PL spectra of ZnO nanotubes.

nated (002) peak indicates that these ZnO nanotubes are preferentially grown in the [0001] direction since these nanotubes are partially vertically aligned on the substrates. The (101), (102), and (103) peaks may be induced by the imperfect vertical alignment as well as other trace nanostructures. We have further verified that these ZnO nanotubes are grown along the [0001] axis by transmission electron microscopy (TEM). Figure 4(b) shows the hollow tubular tip of a ZnO nanotube at low resolution TEM. A high resolution TEM image [Fig. 4(c)] indicates that these ZnO nanotubes are single crystalline with the growth direction (arrows) aligned to the *c* axis of ZnO with lattice spacing of 0.526 nm.

These ZnO nanotubes are then analyzed by photoluminescence (PL). A predominant emission peak at ~380 nm is observed and corresponds to the near-band-edge emission of ZnO attributed to the recombination of the free excitons [Fig. 5(a)]. A weak broad emission at ~600 nm is attributed to intraband defect levels including the singly ionized oxygen vacancy in ZnO. For example, emission of ~520 nm is generated from the recombination of a photogenerated hole with an electron occupying the oxygen vacancy.[19] Raman spectra of these ZnO nanotubes as excited by a HeNe laser (wavelength=632.8 nm) indicate phonon frequencies at 331, 380, 438, and 581 cm^{-1}, which are corresponding to the E_{2H}-E_{2L}, A_{1T}, E_{2H}, and E_{1L} phonon modes of ZnO (Refs. 20 and 21) [Fig. 5(b)]. The detected PL and Raman signals indicate that the ZnO nanotubes maintain the band structures and crystalline structures of the bulk wurtzite ZnO crystals.

In summary, we demonstrate a promising route of growing single crystalline ZnO nanotubes without catalysts and templates by conventional thermal CVD technique. These ZnO nanotubes were grown on the *c* surfaces of ZnO nanorods, as predicted by the theory of nucleation and vapor-solid crystals growth. In principle, the height of these nanorod bases can be minimized so that nanotubes with longer tubular section can be formed.

One of the authors (Y.K.Y.) thanks support from the U.S. Department of Army (Grant No. W911NF-04-1-0029, through the City College of New York) and the Center for Nanophase Materials Sciences sponsored by the Division of Materials Sciences and Engineering, U.S. Department of Energy, under Contract No. DE-AC05-00OR22725 with UT-Battelle, LLC. This work is in part supported by National Science Foundation CAREER award (DMR 0447555).

[1] J. Goldberger, R. He, Y. Zhang, S. Lee, H. Yan, H. J. Choi, and P. Yang, Nature (London) **422**, 599 (2003).
[2] R. Fan, Y. Wu, D. Li, M. Yue, A. Majumdar, and P. Yang, J. Am. Chem. Soc. **125**, 5254 (2003).
[3] Y. Sun, G. M. Fuge, N. A. Fox, D. J. Riley, and M. N. R. Ashfold, Adv. Mater. (Weinheim, Ger.) **17**, 2477 (2005).
[4] G. S. Wu, T. Xie, X. Y. Yuan, Y. Li, L. Yang, Y. H. Xiao, and L. D. Zhang, Solid State Commun. **134**, 485 (2005).
[5] G. K. Mor, K. Shankar, M. Paulose, O. K. Varghese, and C. A. Grimes, Nano Lett. **5**, 191 (2005).
[6] R. Karnik, R. Fan, M. Yue, D. Li, P. Yang, and A. Majumdar, Nano Lett. **5**, 943 (2005).
[7] R. Fan, R. Karnik, M. Yue, D. Li, A. Majumdar, and P. Yang, Nano Lett. **5**, 1633 (2005).
[8] Y. Li, G. W. Meng, L. D. Zhang, and F. Phillipp, Appl. Phys. Lett. **76**, 2011 (2000).
[9] M. H. Huang, Y. Wu, H. Feick, N. Tran, E. Weber, and P. Yang, Adv. Mater. (Weinheim, Ger.) **13**, 113 (2001).
[10] Z. W. Pan, Z. R. Dai, and Z. L. Wang, Science **291**, 1947 (2001).
[11] M. Arnold, P. Avouris, Z. W. Pan, and Z. L. Wang, J. Phys. Chem. B **107**, 659 (2003).
[12] H. T. Ng, J. Han, T. Yamada, P. Nguyen, Y. P. Chen, and M. Meyyappan, Nano Lett. **4**, 1247 (2004).
[13] M. H. Huang, S. Mao, H. Feick, H. Yan, Y. Wu, H. Kind, E. Weber, R. Russo, and P. Yang, Science **292**, 1897 (2001).
[14] X. D. Bai, P. X. Gao, Z. L. Wang, and E. G. Wang, Appl. Phys. Lett. **82**, 4806 (2003).
[15] Z. L. Wang and J. H. Song, Science **312**, 242 (2006).
[16] Z. R. Dai, Z. W. Pan, and Z. L. Wang, Adv. Funct. Mater. **13**, 9 (2003).
[17] J. M. Blakely and K. A. Jackson, J. Chem. Phys. **37**, 428 (1962).
[18] Laboratory Manual on Crystal Growth, edited by I. Tarjan and M. Matrai (Akadémiai Kiadó, Budapest, 1972), pp. 29–30.
[19] K. Vanheusden, W. L. Warren, C. H. Seager, D. R. Tallant, J. A. Voigt, and B. E. Gnade, J. Appl. Phys. **79**, 7983 (1996).
[20] T. C. Damen, S. P. S. Porto, and B. Tell, Phys. Rev. **142**, 570 (1966).
[21] R. P. Wang, G. Xu, and P. Jin, Phys. Rev. B **69**, 113303 (2004).